HALO MITIGATION USING NONLINEAR LATTICES

Kiran G. Sonnad* and John R. Cary
Center for Integrated Plasma Studies and Department of Physics, Boulder, Colorado, CO -80309

Abstract

This work shows that halos in beams with space charge effects can be controlled by combining nonlinear focusing and collimation. The study relies on Particle-in-Cell (PIC) simulations for a one dimensional, continuous focusing model. The PIC simulation results show that nonlinear focusing leads to damping of the beam oscillations thereby reducing the mismatch. It has been well established previously that reduced mismatch leads to reduced halo formation. However, the nonlinear damping is accompanied by emittance growth causing the beam to spread in phase space. As a result, inducing nonlinear damping alone cannot help mitigate the halo. To compensate for this expansion in phase space, the beam is collimated in the simulation and further evolution of the beam shows that the halo is not regenerated. The focusing model used in the PIC simulation will be briefly discussed based on a systematic analysis that has already been done through canonical averaging using Lie transform perturbation theory. This analysis shows that by averaging over a lattice period for a specific arrangement of linear and nonlinear elements, one can reduce the focusing force to a form that is identical to that used in the PIC simulation in an averaged sense, thus providing an equivalence between the model and a realistic system.

INTRODUCTION

Beam halo formation is a major issue limiting the functioning of high current accelerators in a number of current and proposed applications. Some of them include heavy ion fusion, nuclear waste treatment, production of tritium, production of radio isotopes for medical use and spallation neutron sources. The halo is formed by particles that drift far away from the characteristic width of the beam. These particles could get absorbed by the accelerating system causing residual radioactivity. Many of the above applications have a very low tolerance to the number of particles lost, which is about one part in 10^5 to 10^6.

Early studies on beam halo formation included that of O'Connell $et\ al$ [1] who traced the trajectories of various test particles with different initial conditions for a beam in a constant, linear focusing channel. This led to the discovery of "hybrid" trajectories, which undergo a resonant interaction with the breathing mode of the "core". This resonance was later systematically analyzed by Gluckstern [2]. This analysis shows that a one time collimation of the halo is ineffective because the continued resonant interaction causes the halo to almost always regenerate.

The initial part of this paper is based on a more extensive study that uses a combination of nonlinear focusing followed by halo collimation [3]. It relies on the constant focusing channel with no longitudinal variation which is an idealized model that has been extensively used in understanding of formation of the transverse halo in linear focusing systems. The extension of this model to nonlinear focusing is not straight forward and requires more detailed analysis. Moreover, nonlinear focusing itself places a number of restrictions on the performance of the accelerator, for example limiting the dynamic aperture of the machine. Linear focusing systems such as the alternate gradient quadrupole systems contain he Courant-Snyder invariants [4], which reduce the system to an uncoupled set of systems of one degree of freedom. In the presence of higher order components such as sextupoles or octupoles, these invariants are destroyed. Such a system is nonintegrable and has trajectories that are chaotic and poorly confined. The equivalence between a linear alternating gradient system and a continuous focusing force has been analyzed [5, 6, 7, 8]. A similar equivalence that has been extended to nonlinear focusing [9, 10] will be discussed here.

This paper is arranged as follows, the next section consists of a discussion of the relationship between mismatch ratio in linear focusing systems, and the maximum extent of the beam halo. The following section illustrates the process of damping and emittance growth resulting from nonlinear focusing. This will be followed by a study of the effect of halo collimation on a beam in a linear and nonlinear focusing channel respectively. After this, we move over to a brief discussion of the equivalence between a constant, nonlinear focusing model used in the PIC simulations and a realistic focusing system consisting of quadrupoles and sextupoles. The results are summarized in the final section.

HALO AND MISMATCH RATIO

The dependence of the extent of beam halos and the initial beam mismatch has been studied by Wangler $et\ al$, [11], where it has been shown that the maximum dimensionless particle amplitude X_{max}, which is the distance with respect to the matched beam width, can be described by an approximate empirical formula, which is,

$$X_{max} = A + B|ln(\mu)|. \quad (1)$$

Here, A and B are weak functions of the tune depression ratio approximately given by $A = B = 4$ [11], and μ is the initial beam mismatch ratio. This result is not a good estimation for maximum amplitude for μ close to 1. It has also

*now at Stanford Linear Accelerator Center

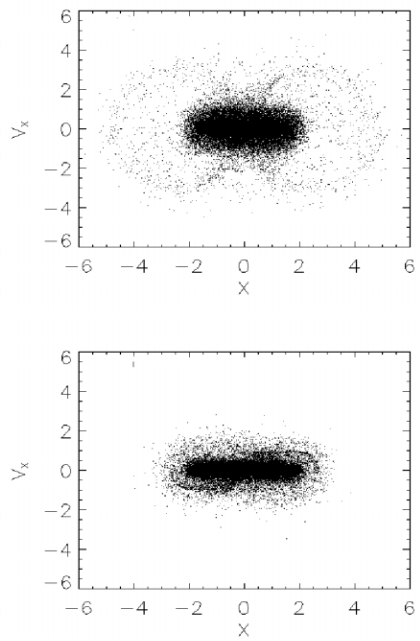

Figure 1: Phase space distribution at minimum rms width for μ = (a) 1.35 (above), (b) 1.02 (below)

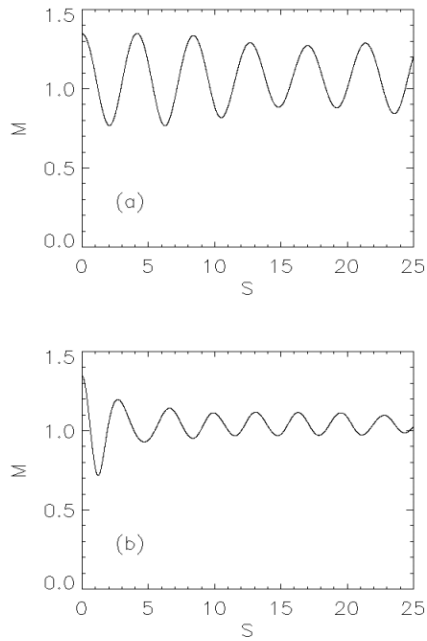

Figure 2: RMS oscillation of beam under (a) linear focusing, (b) nonlinear focusing

been shown [13] that in addition to increased halo extent, the number of halo particles grows with increased initial mismatch ratio. It has also been shown that a better match can be found using nonlinear focusing [12] leading to reduced mismatch.

In Fig 1, we examine the halo generated for beams with two different initial mismatch ratios. The simulation was performed using a radial PIC for a beam with constant focusing and no longitudinal variation. The focusing force was of the form,

$$F = -k_0 r \tag{2}$$

The beam had an initial Gaussian distribution in the transverse position and velocity space. The coordinates represent the normalized phase space variables, $X = x/a_0$ where a_0 is the matched rms beam width as predicted by the rms envelope equation [15], and $V_x = (dx/ds)/\sqrt{k_0}a_0$. The tune depression calculated from the envelope equation was chosen to be 0.1 for all the cases, which implies that the beam is space charge dominated. We used 100,000 particles in all the PIC simulations, which was large enough for the particle distributions to retain the desired azimuthal symmetry required in a radial PIC. The values of the mismatch ratio μ used were (a) 1.35, and (b)1.02 . The runs were performed for about 50 rms oscillations and the distribution was always taken when the rms width of the beam was at a minimum during the rms oscillations. The figures confirm the well known result that reduced mismatch leads to reduced halo formation. The extent of the halo agrees well with the above empirical formula. In a next section, it will be shown that the introduction of nonlinear focusing introduces damping of the beam oscillation thus leading to reduction in the mismatch ratio.

DAMPING OF RMS OSCILLATIONS AND EMITTANCE GROWTH FROM NONLINEAR FOCUSING

Figure 2 shows the oscillation of the rms width of beam scaled to a_0, ie, $M = a/a_0$, for the case of linear and nonlinear focusing respectively. The nonlinear focusing has the form

$$F = -k_1 r - k_3 r^3 \tag{3}$$

The parameters k_0, k_1 and k_3 were related to each other such that $k_0 a_0 = k_1 a_0 + k_2 a_0^3$ and $k_1/(k_2 a_0^2) = 4$. The

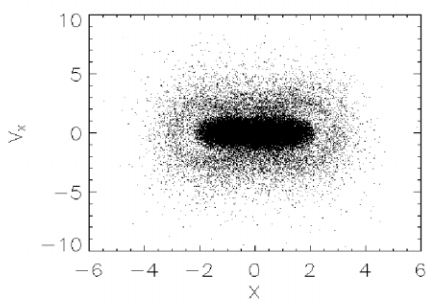

Figure 3: Phase space distribution of the beam with nonlinear focusing

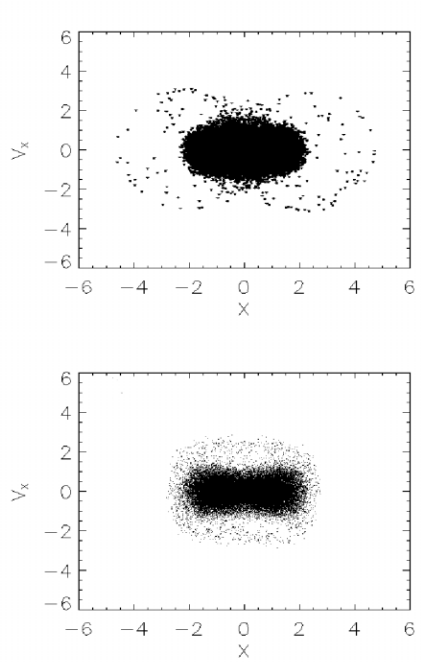

Figure 4: Phase space distribution after collimation for (a) linear focusing (above), (b) nonlinear focusing (below)

initial distributions were identical to each other. The mismatch ratio in the corresponding linear focusing channel was $\mu = 1.35$. It is clear that the nonlinear focusing introduces damping of the rms oscillation thus reducing the mismatch ratio. This phenomenon is well know in various areas of physics as Landau damping.

Figure 3 shows the phase space distribution of the particles subjected to nonlinear focusing under the same conditions described above. The beam was propagated for the same length along the channel as was done for linear focusing shown in Fig 1. The rms width was at its minimum during the end of the oscillations. It is clear that the distribution expands in velocity space. This is due to a transfer of energy stored in the mismatch to the velocity distribution of the particles. The extent in position space is comparable to that obtained in the linear focusing model. Thus, it is clear that nonlinear damping by itself does not control the halo.

COLLIMATION OF HALO WITH LINEAR AND NONLINEAR FOCUSING

It has been well established that a one time collimation for a beam in a linear focusing channel is ineffective [2]. The results in this section confirm these results and provide a reference for comparison with results obtained by collimation followed by nonlinear damping. Collimation in general requires one to identify what region should be regarded as the beam halo. There is no established quantitative definition as yet of a beam halo although recent efforts are being made to quantify such a halo [14]. In the present simulations, the halo was visually identified and collimated in phase space over an ellipse that satisfied the equation $X^2+Y^2/c^2+V_x^2+V_y^2/d^2 = 1$. Here c and d are expressed in units of a_0 and $a_0\sqrt{k_0}$ respectively. The values of c and d were 3.5 and 1.5 respectively for an initial mismatch ratio of 1.35. This resulted in a particle loss of 4.3 percent. A similar procedure was executed for a beam with nonlinear focusing. In this case, the aperture for collimation was different to compensate for the spread in velocity space. That is, c=2.75, d=2.5 and the particle loss was 10.1 percent. It is clear that the halo is eliminated. The collimation was performed by scraping off the particles simultaneously in all dimensions of phase space. While this cannot be realized experimentally, it has been shown that similar results can be produced using a realistic collimation system [3].

Figure 4 shows the phase space distribution of the beam that was evolved for $S = 300$, while the collimation took place after about 15 rms oscillations when the rms width was at its maximum. The mismatch μ was 1.35. It is clear that the halo is regenerated for linear focusing. In order to show the halo particles more clearly, the particles are made to appear a little wider in the first plot. Although the halo intensity is smaller than that seen in Fig. 1, it is large enough to cause radio activity of the walls given that the tolerance to fractional loss in many machines to the number of halo particles is one in $10^4 - 10^5$. In the case of nonlinear focusing, the figure shows that the beam halo is not present. The loss in particles due to collimation is compensated by the absence of a halo. This is because the absence of a halo would increase the acceptance of the machine thus allowing for a higher beam current.

A BRIEF ANALYSIS OF NONLINEAR FOCUSING

In this section, we summarize the results that were derived in [9] and [10]. This analysis provides an equivalence between a constant nonlinear focusing model as was used in the simulations above and a realistic lattice comprising of quadrupoles and sextupoles.

We start by expressing a Hamiltonian in cylindrical coordinates in the absence of space charge forces. This can be obtained from the Lorentz force [9].

$$H = \frac{1}{2}(p_r^2 + \frac{l^2}{r^2}) + \frac{1}{2}\kappa_2(s)r^2\cos(2\theta) \frac{1}{3}\kappa_3(s)r^3\cos(3\theta+\alpha). \quad (4)$$

The variable s is the distance along the axis, which is equivalent to time for constant axial velocity. The momentum in the radial direction is p_r and l is the angular momentum. The values of $\kappa_2(s)$ and $\kappa_3(s)$ depend upon the strength of the quadrupole and sextupole magnets respectively and also the velocity of the particle in the axial direction. The angle α depends upon the relative orientation of the sextupoles with respect to the quadrupoles. We use normalized units in which the charge and mass of the particle are unity.

It is assumed that the Hamiltonian is periodic in s with periodicity S, *ie*, $\kappa_2(s+S) = \kappa_2(s)$ and $\kappa_3(s+S) = \kappa_3(s)$. It is further assumed that the average of $\kappa_2(s)$ and $\kappa_3(s)$ over a period S is zero. That is,

$$\langle \kappa_2 \rangle = \frac{1}{S}\int_s^{s+S} \kappa_2(s)ds = 0 \tag{5}$$

and the same for κ_3. The angle brackets $\langle \cdots \rangle$ denote an average over one period in the rest of this section. With these conditions, κ_2 and κ_3 can in general be represented in the form of a Fourier series as

$$\kappa_2(s) = \sum_{n=1}^{n=\infty} f_n \sin(\frac{2n\pi s}{S}) + \sum_{n=1}^{n=\infty} g_n \cos(\frac{2n\pi s}{S}), \tag{6}$$

and

$$\kappa_3(s) = \sum_{n=1}^{n=\infty} k_n \sin(\frac{2n\pi s}{S}) + \sum_{n=1}^{n=\infty} l_n \cos(\frac{2n\pi s}{S}). \tag{7}$$

Using the above expressions and performing a perturbative canonical averaging procedure, it has been shown [9] that the Hamiltonian can be reduced to the form

$$\begin{aligned} K_3 \;=\; & \frac{1}{2}(P_R^2 + \frac{L^2}{R^2}) + \frac{1}{2}\langle(\kappa_2^{\rm I})^2\rangle R^2 \\ & -\frac{1}{3}\langle\kappa_2^{\rm I}\kappa_3^{\rm I}\rangle R^3\cos(\Theta+\alpha) + \frac{1}{2}\langle(\kappa_3^{\rm I})^2\rangle R^4. \end{aligned} \tag{8}$$

Where (P_R, L, R, Θ) are the transformed, slowly varying phase space variables. The superscript "I" represents an integration over s with a constant of integration chosen such that the integral vanishes when averaged over a period S. This notation will be used in the rest of this section.

In order for K_3 to be independent of Θ, $\langle\kappa_2^{\rm I}\kappa_3^{\rm I}\rangle$ must vanish. It is clear from Eqs. (6) and (7) that one way this can be accomplished is if $\kappa_2(s)$ can be expressed as a pure cosine series and $\kappa_3(s)$ as a pure sine series. Figure (5) represents a practical design for $\kappa_2(s)$ and $\kappa_3(s)$ which exactly satisfies this condition. This is a specific case where the two lattices have equal periodicity. In this case, $\kappa_2(s)$ and $\kappa_3(s)$ are periodic step functions alternating in sign and with opposite parity, which is equivalent to a phase lag of a quarter lattice period with respect to each other. It may be noted that once the Θ dependence is eliminated, the nonlinear force is purely focusing and leads to a positive tune shift. This force is identical to the one used in the PIC simulations. Numerical results have shown [9] that that considerable improvement in the dynamic aperture can be accomplished even if $\langle\kappa_2^{\rm I}\kappa_3^{\rm I}\rangle$ does not completely vanish but is small enough. This is a consequence of improved integrability in the motion because of the weak dependence on the transformed azimuthal coordinate Θ, which leads to the angular momentum to be a conserved quantity over slow time scales. When the dependence on Θ vanishes identically along the channel, the external focusing is the same as that used in the PIC simulations of this paper, at least in an averaged sense. However, to complete the analogy, the perturbation expansion needs to be generalized to include space charge forces.

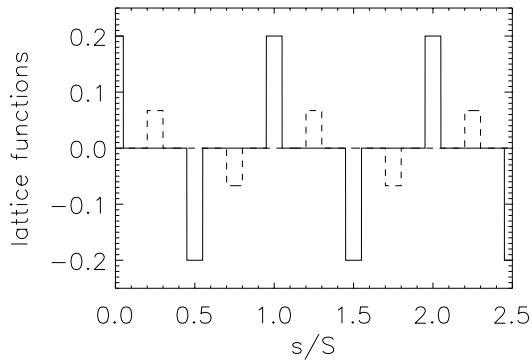

Figure 5: A step function lattice that will lead to a near integrable condition. The shorter steps represent the sextupole function $\kappa_3(s)$ while the higher ones the quadrupole function $\kappa_2(s)$.

When space charge effect are included, the Hamiltonian expressed in Eq (4) is now given by

$$\begin{aligned} H = & \frac{1}{2}(p_r^2 + \frac{l^2}{r^2}) + \frac{1}{2}\kappa_2(s)r^2\cos(2\theta) \\ & +\frac{1}{3}\kappa_3(s)r^3\cos(3\theta+\alpha) + \frac{1}{v_s^2\gamma^3}\phi(r,\theta,s), \end{aligned} \tag{9}$$

where $\phi(r,\theta,s)$ is the space charge electrostatic potential, v_s is the axial velocity and γ is the Lorentz contraction factor. The phase space distribution function f evolves according to the Vlasov-Poisson equation, which is given by,

$$\frac{df}{ds} = \frac{\partial f}{\partial s} + \{H, f\}. \tag{10}$$

The space charge potential is related to f according to Poisson's equation,

$$\nabla^2\phi(q,s) = \int d\mathbf{p} f(\mathbf{q},\mathbf{p},s), \tag{11}$$

where $(\mathbf{q},\mathbf{p})$ are the phase space vectors.

Executing the canonical averaging procedure for this system is a more involved procedure when compared to the previous case where there was no space charge in the Hamiltonian. This has been done in Ref. [10], where it is shown that if the lattice satisfies the condition $\langle\kappa_2^{\rm I}\kappa_3^{\rm I}\rangle = 0$, along with other conditions imposed in the previous analysis for the the beam with no space charge, the above system of equations can be a transformed through a similar canonical averaging procedure that leads to a Hamiltonian given by,

$$\begin{aligned} K = & \frac{1}{2}(P_R^2 + \frac{L^2}{R^2}) + \frac{1}{2}\langle(\kappa_2^{\rm I})^2\rangle R^2 \\ & +\frac{1}{4}\langle(\kappa_3^{\rm I})^2\rangle R^4 + \frac{1}{v_s^2\gamma^3}\phi, \end{aligned} \tag{12}$$

and the corresponding Vlasov-Poisson equations are,

$$\frac{dF}{ds} = \frac{\partial F}{\partial s} + \{K, F\} \tag{13}$$

$$\nabla^2 \phi(\mathbf{Q}, s) = \int \mathbf{dP} F, \tag{14}$$

where F is the phase space distribution function in the transformed, slowly varying coordinate system, and $(\mathbf{Q}, \mathbf{P})$ are the transformed phase space vectors. Since the external focusing component of the Hamiltonian is not dependent on "s" one can obtain equilibrium phase space distribution in the transformed reference frame that satisfies

$$F = F(H(\mathbf{Q}, \mathbf{P})) \tag{15}$$

This translates to a distribution that is close to equilibrium in the original coordinate system, which remains stationary over slow time scales.

The analysis in this section shows that a nonlinear, constant focusing model for a beam with space charge effects is equivalent in an averaged sense to an alternating gradient focusing system with quadrupoles and sextupoles provided the arrangement of the lattice satisfies certain conditions. For this averaging process, it is assumed that the lattice period "S" is sufficiently small compared to a betatron oscillation period.

SUMMARY

This paper first summarizes a more detailed work based on PIC simulations [3] showing that beam halos may be controlled by a combination of nonlinear focusing and collimation. Motivated by the well known results that reduced rms mismatch leads to reduced halo formation, it is first shown that nonlinear focusing damps the rms oscillations of the beam thereby reducing its mismatch. However, the damping is accompanied by emittance growth causing the phase space distribution to expand and populate particles well beyond the width of the original phase space distribution. To compensate for this emittance growth, the high amplitude particles are scraped off and it is shown that continued evolution of the beam does not reproduce a halo.

This is followed by a discussion of the nonlinear focusing used in the PIC simulations. Summarizing the work in Refs. [9], [10], the discussion shows that an equivalence exists between a nonlinear, constant focusing model as that used in the PIC simulations and an alternating gradient focusing system. The analysis of the nonlinear focusing is important because the extension to a continuous focusing model from an alternating gradient one is not straight forward for such nonlinear transport systems. The analysis shows the certain conditions between the arrangement of the quadrupoles and sextupoles need to be satisfied in order to produce an equivalent constant nonlinear focusing channel. In general, a system that is closer to a constant focusing model implies improved integrability which in turn leads to a larger dynamic aperture.

This work could find applications in various high current linacs where beam halos are an issue. To include nonlinear components in rings requires more detailed analysis due to the effect of resonances and beam instabilities. However, it has been shown here that the nonlinear damping is a transient process that takes place in 1-2 rms oscillations. Once the collimation is achieved, the beam could be adiabatically matched to a linear focusing section. Such a matching procedure has been studied by Batygin [16]. The possibility of realizing such a procedure experimentally would greatly contribute toward improving the performance of accelerators using high intensity beams.

ACKNOWLEDGMENTS

This work was supported by the U.S. Department of Energy under Grand No. DE-FG03-95ER40926

REFERENCES

[1] J. S. O'Connell and T.P. Miller and R. S. Mills and K. R. Crandall, 1993, Proceedings of the 1993 Particle Accelerator Conferemce, Washington, DC, edited by S. T. Corneliussen

[2] R. L. Gluckstern, Phys Rev. Lett., '73', pp 1247 (1994).

[3] K. G. Sonnad and J. R. Cary "Control of Beam Halo Through Nonlinear Damping and Collimation", to be published in Phys. Rev. ST/AB.

[4] E. D. Courant and H. S. Snyder, Annals of Physics,'3' pp 1 (1958)

[5] P. Channel, Phys. Plasmas, '6', pp 982 (1999)

[6] R. C. Davidson and H. Qin and P.J. Channell, Phys. Rev. ST Accel. Beams, '2' pp 074401 (1999)

[7] R. C. Davidson and H. Qin, Phys. Rev. ST Accel. Beams, '4', pp 104401, (2001)

[8] S.I. Tzenov and R. C. Davidson, Phys. Rev. ST Accel. Beams, '5', pp 021001 (1999)

[9] K. G. Sonnad and J. R. Cary, Phys. Rev E, '69' pp056501 (2004)

[10] K. G. Sonnad and J. R. Cary, in preparation, to be submitted to Phys. Plasmas

[11] T.P. Wangler and K. R. Crandall and R. Ryne and T. S. Wang, Phys. Rev. ST Accel and Beams, '1', pp 084201 (1998)

[12] Y. K. Batygin, Phys. Rev. E, '57', pp 6020, (1998)

[13] M. Ikegami and H. Okamoto, Jpn. J. Appl. Phys., pp 7028, (1997)

[14] C. K. Allen and T. P. Wangler, Phys. Rev. ST Accel and Beams, '5', pp 124202, (2002)

[15] Thomas. P. Wangler, "RF Linear Accelerators", Wiley Series in Beam Physics and Accelerator Technology (1998)

[16] Y. K. Batygin, Phys. Rev. E, '54' pp 5673, (1996)